Combustion and Flame 156 (2009) 1950–1956

Contents lists available at ScienceDirect

Combustion and Flame

journal homepage: www.elsevier.com/locate/combustflame

Ammonia chemistry in a flameless jet

Mariusz Zieba [a,*], Anders Brink [b], Anja Schuster [a], Mikko Hupa [b], Günter Scheffknecht [a]

[a] Institute of Process Engineering and Power Plant Technology, University of Stuttgart, Pfaffenwaldring 23, D-70569 Stuttgart, Germany
[b] Process Chemistry Centre, Åbo Akademi University, Biskopsgatan 8, 20500 Åbo, Finland

ARTICLE INFO

Article history:
Received 7 January 2009
Received in revised form 1 March 2009
Accepted 6 July 2009
Available online 5 August 2009

Keywords:
Flameless combustion
Fuel-NO_x
Ammonia conversion

ABSTRACT

In this paper, the nitrogen chemistry in an ammonia (NH_3) doped flameless jet is investigated using a kinetic reactor network model. The reactor network model is used to explain the main differences in ammonia chemistry for methane (CH_4) containing fuels and methane-free fuels. The chemical pathways of nitrogen oxides (NO_x) formation and destruction are identified using rate-of-production analysis. The results show that in the case of natural gas, ammonia reacts relatively late at fuel lean condition leading to high NO_x emissions. In the pre-ignition zone, the ammonia chemistry is blocked due to the absence of free radicals which are consumed by methane–methyl radical (CH_3) conversion. In the case of methane-free gas, the ammonia reacted very rapidly and complete decomposition was reached in the fuel rich region of the jet. In this case the necessary radicals for the ammonia conversion are generated from hydrogen (H_2) oxidation.

1. Introduction

Flameless oxidation technology (FLOX®), has already demonstrated great potential in reducing thermal NO_x formation [1–3] while burning natural gas. In contrast to combustion within classical flames, temperature peaks are avoided due to the high internal recirculation of combustion products. Recent works on FLOX® technology are focussed on its adaptation to combust low calorific value gases generated from the biomass [4]. During air gasification of biofuels, the fuel nitrogen is released mainly as ammonia or hydrogen cyanide (HCN) in concentration up to thousands ppm. These compounds are formed as a result of thermal destruction of proteins and amino acids contained in the biomass [5,6]. During combustion of such gases, the nitrogen-containing species may be oxidised to NO_x or they may be reduced to N_2. The selectivity of this process depends on the gas composition, temperature and mixing of the reactants. The main chemical routes of NO_x formation from fuel nitrogen were established by Miller and Bowman [7]. There are several publications in literature dealing with the ammonia chemistry related to high temperature conditions in flames [7–12], as well as related to moderate temperatures which can occur in fluidized bed combustion [13] or in post-combustion processes [14].

The conditions in flameless combustion are different from those mentioned above. Due to the high momentum of the oxidizer jet, internal recirculation of the hot combustion products occurs. These hot products are partially mixed with the fuel and oxidizer before the mixture ignites. As a result, there is no identifiable flame front. The reactants are strongly diluted and the temperature field is homogeneous without high peaks. Schuster et al. [15] observed that the ammonia conversion in such jets depend strongly on the gas composition: the conversion of ammonia to NO_x in gases containing only carbon monoxide (CO) and H_2 is very small compared to gases containing hydrocarbons. According to the authors knowledge no one has yet modelled NH_3 conversion in ammonia-doped flameless jets.

The goal of this paper is to explain the main differences in nitrogen chemistry between methane-containing and methane-free ammonia-doped gases in flameless jets. A reactor network models with detailed reaction mechanisms are used for the modelling. In order to establish the main reactor model parameters such as residence time, oxidizer/fuel mixing and recirculation ratio of the hot product gases, computational fluid dynamics (CFD) modelling of the combustion chamber was performed. Three different ammonia-doped gaseous mixtures have been simulated and compared against previously published experimental data [15].

2. Experimental background

All experimental data used in this paper to validate the modelling results were taken from Schuster et al. [15]. The objective of the experiments was to investigate the ammonia oxidation and thus the conversion of volatile fuel nitrogen to NO_x under flameless conditions. The experiments were performed using a 20 kW FLOX®-burner. The burner had been originally developed for natu-

* Corresponding author. Fax: +49 711 685 63491.
E-mail address: zieba@ivd.uni-stuttgart.de (M. Zieba).

0010-2180/$ - see front matter © 2009 The Combustion Institute. Published by Elsevier Inc. All rights reserved.
doi:10.1016/j.combustflame.2009.07.002

ral gas (NG) and was subsequently modified to combust low calorific value gases. The test rig is shown in Fig. 1.

Different gas mixtures were used in the experiments of Schuster et al. Three of them have been selected for the model validation. The composition of all selected gases and their calorific values are summarised in Table 1. The first fuel is a natural gas (NG) with a lower heating value of 36 MJ/m^3 i.N. The natural gas contains mainly methane and very small amounts of ethane (C_2H_6), carbon dioxide (CO_2) and nitrogen (N_2). The amount of higher hydrocarbons can be assumed to be negligible. The next two gases are synthetic low calorific value (LCV) mixtures provided by a mixing station. Methane-containing syngas (MCS) represents a gas generated from biomass air blown gasification. The third tested gas is a methane-free syngas (MFS). Ammonia and hydrogen cyanide are the main NO_x precursors created during the gasification of biomass [5,6]. In order to investigate the fuel nitrogen conversion, ammonia at different concentrations were added to the fuel stream [15]. The concentration of NH_3 was varied between 0 and 900 ppmv$_{(dry)}$ for NG, 0–750 ppmv$_{(dry)}$ for methane-free syngas, and 0–650 ppmv$_{(dry)}$ for methane-containing syngas. The value is related to the ammonia concentration in the gas and the combustion air mixture. All experiments were carried out at a firing capacity of 18 kW, a temperature of approximately 1000 °C and with 50% excess air.

With no ammonia added to the fuel stream, the emitted NO concentration was 50 ppmv$_{(dry)}$ when natural gas was the fuel, whereas for other tested LCV gases the value of NO in flue gas was about 10 ppmv$_{(dry)}$. For all of the tested gases, the NO emission increases with increasing ammonia concentration. In the cases of natural gas and methane-containing syngas the conversion of NH_3 to NO was found to be similar and relatively high. In contrast, the NO emission while burning methane-free gas was significantly lower. It is an indication that the ammonia chemistry in flameless combustion is strongly influenced by the composition of the fuel gas, particularly with respect to the hydrocarbon content in the fuel. A compilation of the selected results of Schuster et al. are shown in Fig. 2.

3. Numerical modelling

The numerical modelling of the combustion process was performed using the commercial Chemkin 4.1 software package. The Åbo Akademi (*ÅA*) [16] kinetic reaction scheme was used to simulate the chemistry occurring in the combustion chamber. The *ÅA* mechanism was created for the simulation of the gas phase combustion of biomass-derived gases under moderate temperature conditions. The scheme is based on the mechanism of Glarborg et al. [17,18] and Miller and Glarborg [19]. The mechanism has been validated in the past and applied to a number of conditions giving satisfactory predictions of nitrogen and hydrocarbon combustion kinetics over a wide range of temperatures and air–fuel ratios [20–25]. Since the flameless combustion of ammonia-doped low calorific value gases occurs at moderate temperatures and

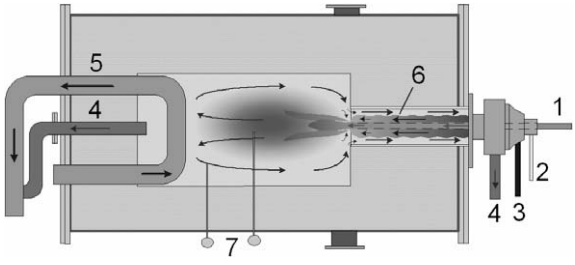

Fig. 1. Scheme of FLOX®-burner test rig (1 – LCV gas, 2 – natural gas, 3 – combustion air, 4 – flue gas, 5 – cooling, 6 – recuperator pipe, 7 – thermocouples).

Table 1
Composition of the selected gases.

	NG	MFS	MCS
CH_4 (vol%)	95.6	–	6.5
C_2H_6 (vol%)	2.4	–	–
H_2 (vol%)	–	25.0	8.6
CO (vol%)	–	18.0	8.8
CO_2 (vol%)	0.4	15.0	15.6
N_2 (vol%)	1.6	42.0	60.5
LCV (MJ/m^3 i.N.)	36.1	5.0	4.4

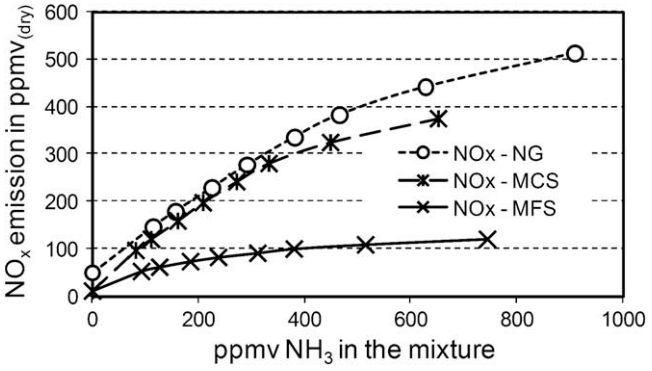

Fig. 2. NO_x concentration in the flue gas for three different gases as a function of ammonia concentration in the combustion mixture (fuel and combustion air).

the composition of the MFS and MCS fuels are similar to bio-derived fuels, the *ÅA* mechanism was considered a suitable scheme. The *ÅA* kinetic scheme involves 371 elementary gas phase reactions for the oxidation of H_2, CO, light hydrocarbons (C_1 and C_2) and methanol (CH_3OH). The mechanism also takes into account the reaction subsets of nitrogen pollutants such as the oxidation of NH_3 and HCN as well as sub-mechanisms describing the interactions between hydrocarbons and nitrogen-containing species.

To see to what extent the conclusions of this work depend on the chosen reaction scheme, the results obtained using *ÅA* mechanism were compared with results from the well established GRI-Mech 3.0 kinetic mechanism [26]. Although GRI-Mech 3.0 mechanism is not well suited for NH_3 oxidation, satisfactory results of ammonia-doped methane/air flames modelling using this mechanism have been reported in the past [8]. Moreover, the GRI-Mech 3.0 has already been used for the modelling of nitrogen pollutants during flameless combustion of methane [27]. The GRI-Mech 3.0 has been specifically designed to describe methane and ethane combustion at high temperatures [28].

3.1. Modelling approach

Fig. 3a illustrates the flow field (axial velocity) inside the modelled combustion process. The fuel and preheated air are introduced with high velocity forming a jet. The jet develops taking the product gases from its environment back into the stream. The mixing between the air, fuel and combustion products occurs continuously along the jet.

The model described in this work considers detailed reaction mechanisms implemented in a network of plug flow reactors (PFR). Fig. 3b shows the isothermal PFR's connected in series, which represent the jet propagation in the combustion chamber. In order to simulate the mixing processes two different approaches for the mixing of fuel with air have been used. Similar approaches have been successfully employed in different Selective Non-Catalytic Reduction (SNCR) and reburn modelling studies [29,30].

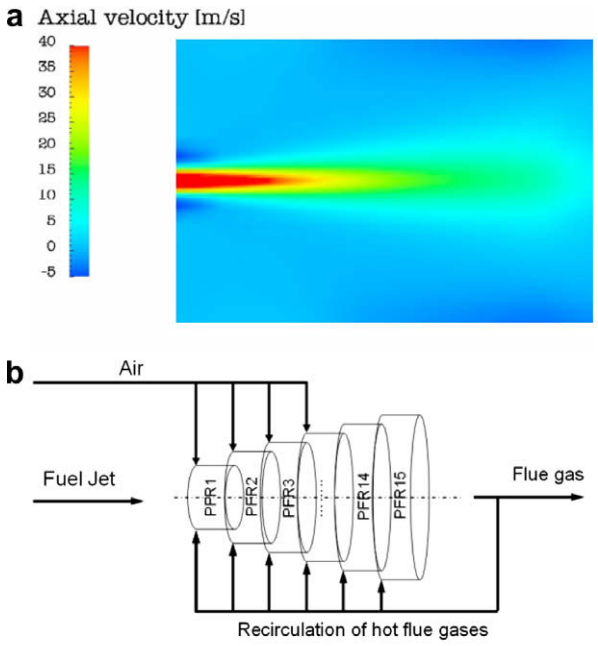

Fig. 3. Principle of the flameless jet model; (a) flow field in the combustion chamber and (b) reactor model air-into-fuel mixing approach.

Because of the high velocity and volume flow of the preheated air, the first assumption was to treat the air as the main stream and therefore to introduce the ammonia-doped fuel stepwise into the air jet. This approach will be called here the fuel-into-air mixing approach.

The second approach, the air-into-fuel mixing approach, assumes the entrainment of the oxidizer into the fuel stream. The amounts of entrained oxidizer mass flows into the PFR's were discretely distributed in equal amounts.

It has to be mentioned that the mixing between oxidizer and fuel occurs only along a part of the jet, which means the fuel or oxidizer is entrained only to some of PFR's in the model. The method of estimating the mixing length will be described in Section 3.2.

The recirculation of product gases is essential for flameless oxidation, whereby the combustion products are entrained into the jet, diluting the combustion environment and influencing the chemical reactions taking place and thus changing the end-flue gas composition. The calculations were carried out iteratively by using the end-flue gas composition from the preceding iteration as the input value for the composition of recirculated gases. This procedure was repeated until the system reached a steady state solution. The part of the jet where the oxidizer is still mixing with the fuel is discretized using 2 cm long reactors, whereas the remaining length is discretized using 10 cm long reactors. Additionally, the length of the last reactor has been set up in such a way that the complete residence time in the system is 2 s. This should ensure enough time to complete the combustion and decrease the pool of free radicals in the recirculated product gas. The stream of recirculated gases was assumed to be non-reactive.

3.2. Parameters estimation – CFD modelling

In order to estimate the main parameters of the reactor network model, such as the residence time for the PFR's, the mixing distance and the distribution of the recirculated gases, CFD modelling using the commercial code FLUENT was carried out. The simple modelling of the combustion chamber was done using the 4-step global hydrocarbon chemistry model of Jones and Lindstedt [31]. The turbulence–chemistry interaction was modelled applying the Eddy-Dissipation–Combustion Model of Magnussen and Hjertager [32]. The standard k–ε model has been used for the turbulence modelling.

The modelling results are shown in Fig. 4. In the reactor network model, every PFR represents a certain part of the propagating jet (1-D model). Therefore the residence time for each reactor could be estimated based on the average velocity of the propagating jet at a certain position. The velocity is presented in Fig. 4a. The velocity decreases with increasing mass flow of the jet. Fig. 4b shows the mass flow of the jet. The difference between the input mass flow and the local mass flow of the jet indicate the local dilution caused by the internal recirculation of the combustion products. The recirculation mass flow was calculated as the difference between the average mass flow for a certain reactor, taken from the CFD results, and the mass flow transported from the preceding reactor. The mixing between fuel and oxidizer takes place only along a part of the jet. The location where mixing is considered to be complete was estimated using the mixture fraction factor. The mixture fraction measures the fuel/oxidizer ratio and can be written in terms of the mass fraction as

$$\xi = \frac{Y_i - Y_{i,ox}}{Y_{i,fuel} - Y_{i,ox}} \tag{1}$$

where Y_i is the elemental mass fraction for element i. The subscript *ox* and *fuel* denotes the value at the oxidizer or fuel stream inlet, respectively. The values of stoichiometric mixture fractions for NG, MCS and MFS were 0.058, 0.48 and 0.45, respectively.

It was assumed that the mixing process is complete when the mixture fraction factor on the axis of the simulated combustion chamber (using CFD code) has reached the value of the stoichiometric mixture fraction.

4. Results and discussion

The development and adaptation of the flameless technology for low calorific value gases creates a uniform combustion environ-

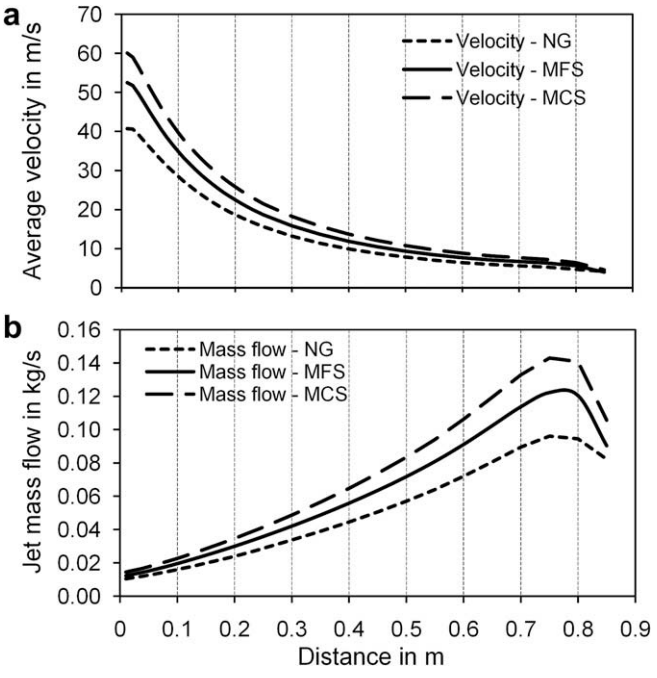

Fig. 4. Results of the CFD modelling of the combustion chamber for three different gaseous mixtures; (a) average velocity of the jet and (b) mass flow rate of the jet.

ment that allows comparison of ammonia behaviour in gases with significantly varying composition. The lower heating value of the fuel gas varies from 4.4 to 36 MJ/m^3 i.N. in these studies. Due to the burner flexibility and combustion stability, the comparison of ammonia decomposition can be done under very similar conditions for all of the tested fuels. The high dilution of the reaction zone caused by the recirculation of hot flue gases significantly decreases the temperature peaks in the combustion chamber [1]. Therefore, the combustion of the studied fuels occurs at very similar intermediate temperature conditions. Moreover, the hot recirculated gases include nitrogen oxides that influence the nitrogen chemistry in the jet.

4.1. Kinetic schemes and the effect of mixing

The analysis of modelling studies of the ammonia conversion using three different gas mixtures under flameless combustion conditions was performed. In order to validate the reactor network models, the predicted NO_x concentration values are compared with the experimental results of Schuster et al. [15]. The *ÅA* and GRI-Mech 3.0 kinetics mechanisms were used for modelling. However, the GRI-Mech 3.0 mechanism was used only together with the air-into-fuel mixing approach.

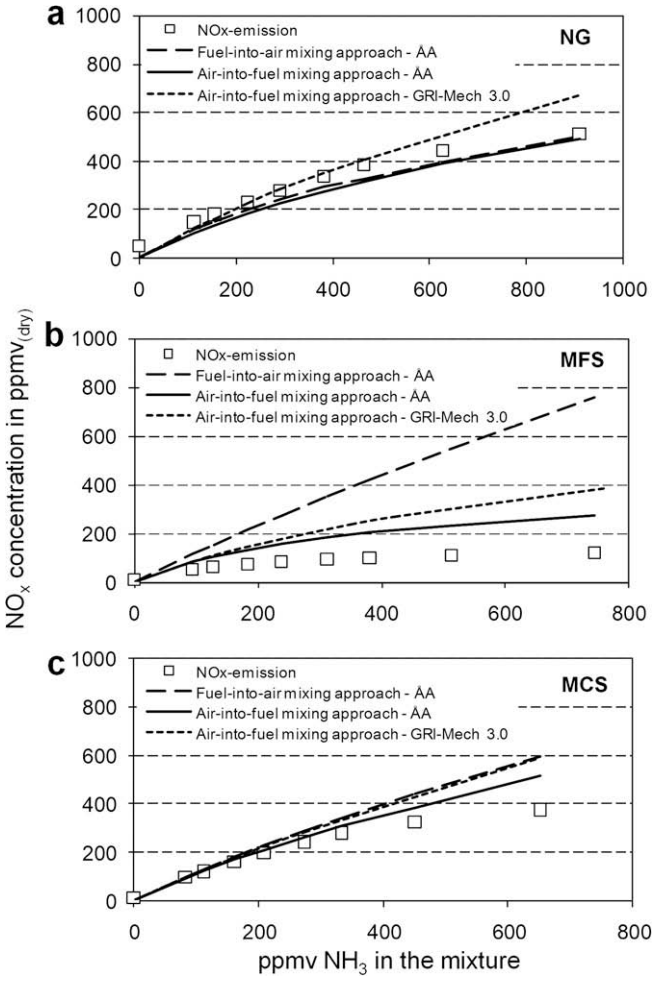

Fig. 5. Comparison between experimental results (Schuster et al. [15]) and model results versus inlet ammonia concentration; (a) results for ammonia-doped natural gas, (b) results for ammonia-doped methane-free syngas, and (c) results for ammonia-doped methane-containing syngas. Experimental conditions: $P = 18$ kW, $T = 1000$ °C, 50% excess air.

4.1.1. Modelling using the ÅA mechanism

The modelling results are shown in Fig. 5. In the case of ammonia-doped natural gas, both of the mixing models using the *ÅA* mechanism predicted the NO_x concentration very well over the whole range of ammonia input as shown in Fig. 5a. Here production of the nitrogen oxides occurs only via fuel-NO reaction pathways. Fig. 5c shows the modelled NO_x concentration for methane-containing syngas. The calculated values were slightly higher than the measured ones, whereas the model with the air-into-fuel mixing approach resulted in better agreement with the measured data. With decreasing methane content in the fuel, the overprediction of the NO_x with the fuel-into-air mixing approach increased. The predicted NO_x concentrations for the methane-free syngas were strongly overestimated as shown in Fig. 5b. Only the model with the air-into-fuel mixing approach was able to predict the trends for all experimentally tested gas compositions. For natural gas and methane-containing syngas, the modelled conversion of ammonia to NO_x was relatively high compared to the methane-free syngas, which was in good agreement with the measurements.

The main difference between the two mixing approaches is the local stoichiometric ratio λ along the modelled jet. In the case of the fuel-into-air approach, the entire combustion process takes place under overstoichiometric conditions. In the case of the air-into-fuel mixing approach, there exist substoichiometric conditions at the entrance and overstoichiometric conditions at the outlet. Therefore, the ammonia in the fuel reacts under a broad spectrum of conditions, going from very fuel rich, through to fuel lean, and to conditions of full mixing. This seems to be essential for the modelling of ammonia chemistry in the flameless jet.

4.1.2. Modelling using the GRI-Mech 3.0 mechanism

Additional calculations were carried out using the GRI-Mech 3.0 mechanism together with the air-into-fuel mixing approach. Fig. 5 shows that by using this kinetic scheme, the reactor network model was able to predict the trends satisfactorily: i.e. showing lower concentration of NO_x in the case of methane-free gas. However, in all cases the model overestimated the NO_x emissions. The discrepancy increased with increasing ammonia concentration in the fuel. The possible reasons for the discrepancies are discussed below.

4.2. Nitrogen-containing species behaviour along the jet

The proposed model with the air-into-fuel approach of mixing was able to predict the trends of ammonia conversion to NO_x quite well. Therefore, the analysis of the computed results for natural gas and methane-free syngas was performed in order to describe the chemical processes of ammonia decomposition and NO_x creation along the flameless jet.

In Fig. 6, profiles of the normalised fluxes of the main nitrogen-containing species and combustibles have been plotted as a function of the distance from the burner nozzle. Fig. 6a–d presents the results obtained using the *ÅA* kinetic scheme, whereas Fig. 6e–h displays the calculated results using the GRI-Mech 3.0 mechanism. Fig. 6a shows the normalised flux profiles of nitrogen-containing species while burning natural gas. The results indicate that along the first 20 cm ammonia does not react. At the same time the recirculated NO coming from the flue gas is slowly consumed. Since the recirculated part of NO has been extracted from the main flux, its negative value means, that the recirculated NO is consumed faster than it is produced at the burner entrance. The almost constant value of NO and NO_2 flux indicates, that the part of the NO is not reduced to N_2 but it is converted to NO_2.

Fig. 6b shows the profile of combustibles, while burning natural gas. When the methane ignites, ammonia rapidly decomposes and the initially created NO_2 reduces back to NO. These processes take place in the part of the jet where all of the combustion air has al-

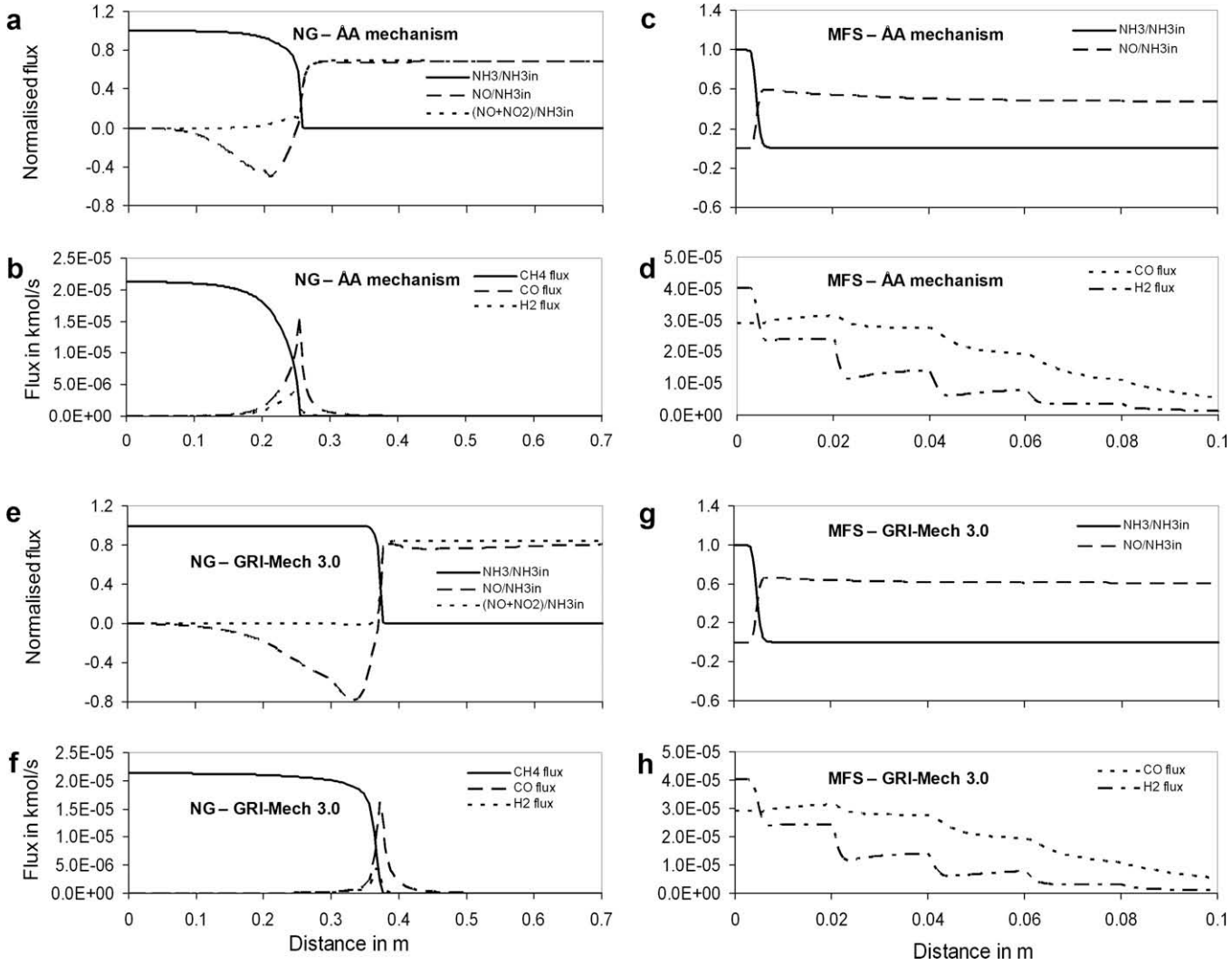

Fig. 6. Predicted flux profiles as a function of distance from burner nozzle. The fluxes of NH_3, NO and (NO + NO_2) have been normalised to the incoming flux of ammonia; in all cases the recirculated part of the flux has been removed from the total flux; (a) profile along the jet of normalised flux of NH_3, NO and (NO + NO_2) for ammonia-doped natural gas – *ÅA* mechanism; (b) flux of CH_4, CO and H_2 along the jet for natural gas – *ÅA* mechanism; (c) profile of NH_3 and NO normalised flux for methane-free syngas – *ÅA* mechanism; (d) profile of CO and H_2 flux for methane-free syngas – *ÅA* mechanism; (e) profile along the jet of normalised flux of NH_3, NO and (NO + NO_2) for ammonia-doped natural gas – GRI-Mech 3.0; (f) flux of CH_4, CO and H_2 along the jet for natural gas – GRI-Mech 3.0; (g) profile of NH_3 and NO normalised flux for methane-free syngas – GRI-Mech 3.0; and (h) profile of CO and H_2 flux for methane-free syngas – GRI-Mech 3.0. Conditions: 310 $ppmv_{(dry)}$ NH_3, $T = 1000$ °C, 50% excess air.

ready been introduced into the fuel stream. The conditions are overstoichiometric.

In quite the opposite manner, the ammonia contained in the methane-free syngas reacts rapidly after the gas nozzle under substoichiometric condition as shown in Fig. 6c. Therefore, the conversion of NH_3 to NO is much lower. Since the NO_2 was not present in significant concentrations in this case Fig. 6b and g shows only the behaviour of the NO. The profile of combustibles shown in Fig. 6d indicates that the combustion process is limited by mixing. Due to the assumption of discrete oxidizer entrainment, the flux of CO and H_2 decreases stepwise.

Similar results were observed using the GRI-Mech 3.0 mechanism. However, some differences could be noticed. The first difference was the longer ignition delay for NG, as shown in Fig. 6f, compared to that obtained using the *ÅA* mechanism. This caused more NO to be oxidised to NO_2, resulting in higher final NO_x emissions as shown in Fig. 6e. Another possible reason for the higher predicted NO_x emissions is the favouring of HNO over N formation in the mechanism. This was observed by Sullivan et al. [8], when studying non-premixed methane/air flames when using GRI-Mech 3.0.

The fluxes of combustibles for MFS, shown in Fig. 6h, were identical for both kinetic schemes. The behaviour of nitrogen species, shown in Fig. 6g, was also similar, although the GRI-Mech 3.0 showed higher NH_3 to NO_x conversion.

Both of the mechanisms overestimated the measured values for MCS and MFS. The differences were particularly big for MFS. The *ÅA* and GRI-Mech 3.0 schemes with the air-into-fuel mixing approach overestimated the results by a factor of two and three, respectively. A possible source for these errors could be the simplification of the turbulent mixing. Fig. 6c and g shows that the whole ammonia decomposition takes place in the first reactor. Therefore, the description of the mixing in the zone directly after the burner nozzle is of key importance.

For the NG the errors were much smaller, because the process was limited by the chemistry and the discretization of the mixing in the model was not as crucial. Because of the high speed of the jet and relatively long delay in ignition all reaction were taking place at the fuel lean side of the mixture. Therefore, also the fuel-into-air mixing model was able to predict the values correctly.

Another reason for the overestimation of the measured NO_x emissions for the MCS, particularly at higher concentrations of

ammonia could be missing reaction pathways in the kinetic mechanisms. Dean and Bozzelli [33] have identified an additional pathway of relevance in ammonia oxidation in the temperature range 1000–1300 K via the intermediate methylamine. Koger and Bockhorn [34] later showed that this pathway does play a role in ammonia oxidation at conditions where methane is present. However, Koger et al. showed that this pathway contributes only to 10% or less of ammonia conversion leading to additional HCN formation. Therefore, it is unlikely that the methylamine pathway would have a significant influence on the overall conclusions of our model calculations using the *ÅA* mechanism.

4.2.1. Reaction path analysis

A rate-of-production (ROP) analysis was performed in order to identify the main reaction routes for the formation and decomposition of nitrogen-containing species. The ROP analysis was performed using the *ÅA* mechanism, since there were no significant differences found in the main nitrogen species behaviour and the results using the *ÅA* mechanism were in better agreement with the measured data. Moreover, the analysis was carried out only for the reactors which are representative of the processes taking place along the jet. For the natural gas fuel, two reactors have been chosen. The first one corresponds to the distance, where the methane decomposition occurs very slowly and the nitrogen oxide is converted to NO_2. The second reactor corresponds to the place, where methane ignites and ammonia is rapidly consumed. In the case of methane-free syngas, the first reactor was essential for the NO_x formation. The main reaction pathways were drawn based on time integration of rate-of-production under ideal plug flow conditions. The most important pathways are indicated in Figs. 7 and 8 with thicker arrows.

In the pre-ignition zone of the natural gas/air flameless jet the NO–NO_2 conversion is taking place. Methane slowly converts to methyl radicals via the following reactions:

$$CH_4 + H \leftrightharpoons CH_3 + H_2 \quad (2)$$

$$CH_4 + O \leftrightharpoons CH_3 + OH \quad (3)$$

$$CH_4 + OH \leftrightharpoons CH_3 + H_2O \quad (4)$$

Those three reactions consume most of the H, O and OH radicals occurring in the jet. The CH_3 radical undergoes further reactions which via formaldehyde (CH_2O) and formyl radical (HCO) leading to hydroperoxyl radical (HO_2) formation. The HO_2 radical is responsible for the conversion of previously recirculated NO to NO_2 via the reaction:

$$NO + HO_2 \leftrightharpoons NO_2 + OH \quad (5)$$

At the same time, ammonia conversion does not proceed because of the lack of radicals able to react with NH_3 at 1000 °C.

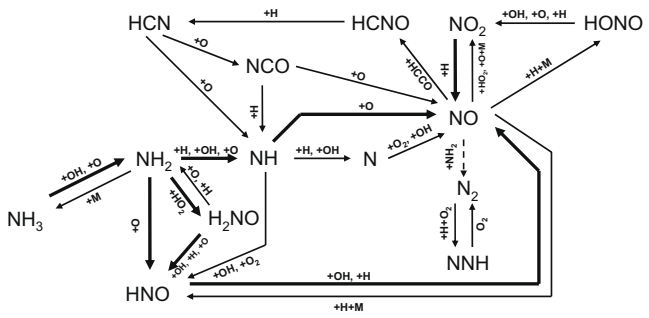

Fig. 7. Main chemical reaction pathways of NO creation and reduction in a flameless jet of ammonia-doped natural gas.

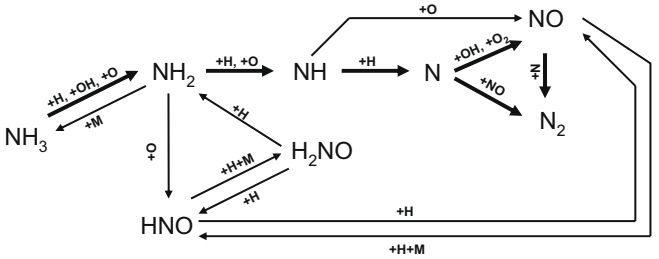

Fig. 8. Main chemical pathways of NO creation and reduction in flameless jet for ammonia-doped methane-free syngas.

Mancini et al. [27] have also reported the formation of NO_2 in the flameless combustion of methane/air mixture. However, they found that besides reaction (5), a reaction:

$$NO + O + M = NO_2 + M \quad (6)$$

generates around two-thirds of the total NO_2 produced, whereas in this work the contribution of this reaction was only minor.

As the methane ignites, ammonia decomposition progresses rapidly. In this part of the jet all of the combustion air has already been introduced into the fuel stream. The conditions are overstoichiometric. The abundant oxygen causes that almost all of the NH_3 is converted to NO. This makes the process different to the classical flames. Sullivan et al. [8] have investigated the ammonia conversion and NO_x formation in non-premixed methane-air flames. They found that ammonia is decomposed and NO is formed mainly in the ignition region, which occurs at the border between fuel reach and fuel lean mixture. In the flameless process, the high velocity of the jet causes the combustion mixture to be fuel lean when igniting. The main chemical pathways related to nitrogen conversion are shown in Fig. 7. The major part of the NO is created via oxidation of imidogen (NH), the nitroxide radical (H_2NO) and nitrosyl hydride (HNO). Although some reaction pathways via HCN are found active, they have a very small influence on the overall NO concentration. The NO_2 initially created in the pre-ignition zone is now converted back to NO. Some additional creation of NO_2 via HONO was found. The reduction of NO to N_2 during the ignition time was almost negligible.

The process of NH_3 decomposition and NO_x creation in the case of methane-free syngas is different to that observed for the natural gas. According to the model, all of the ammonia reacts rapidly in the substoichiometric region of the jet. The hydrogen contained in the fuel ignites directly after the nozzle and releases enough radicals to start the ammonia decomposition. The released radicals are not completely consumed by other combustibles and easily react with NH_3. The main chemical paths leading to NO creation and reduction are shown in Fig. 8.

The main part of the NO is created via oxidation of nitrogen radicals (N) which are formed via the reaction:

$$NH + H \leftrightharpoons N + H_2 \quad (7)$$

Simultaneously the same radicals react with nitrogen oxide forming N_2.

$$N + NO \leftrightharpoons N_2 + O \quad (8)$$

This reduction mechanism was found to be very important. The pathways via H_2NO and HNO are also active but the net contribution to NO creation is relatively small.

5. Conclusions

The presented kinetic modelling study shows the fate of ammonia and nitrogen-containing species in a flameless jet for different

gaseous fuels mixtures. Depending on the gas composition, there can be a large difference in the conversion of NH_3 to NO_x.

In the case of flameless natural gas combustion, the methane ignites with delay around the location where the oxidant is already completely mixed with the fuel. Before the ignition occurs, the ammonia conversion is inhibited due to the absence of radicals which are instead consumed by methane–methyl radical conversion. Recirculated NO is converted to NO_2 in this part of the jet. After methane ignition, ammonia oxidises mostly to NO.

In the flameless jet of methane-free gas, ignition occurs rapidly and ammonia decomposes in the substoichiometric region of the jet. The radicals needed for ammonia decomposition are generated from hydrogen oxidation. In contrast to the natural gas jet the radicals are not completely consumed by other combustibles. The reduction of NO to N_2 is very pronounced and result in significantly lower nitrogen oxides emissions.

Since the ignition delay depends on the fuel composition, the high velocity of the jet and the strong recirculation can lead to crucial changes in local stoichiometry under which the mixture ignites. The longer ignition delay the higher amount of air and recirculated gases are mixed with the fuel when igniting. Since the ignition zone is not stabilized in the flameless combustor, it can significantly influence the ammonia to NO_x conversion. The modelling results also showed that for the ammonia-doped fuel, a correct mixing approach is critical in order to successfully predict the concentration of nitrogen-containing species under flameless oxidation conditions.

Although, the choice of kinetic scheme had an influence on the final NO_x prediction, the results show similar behaviour of the main nitrogen species along the jet. The model is able to accurately predict the trends using both the *ÅA* and the GRI-Mech 3.0 kinetic mechanisms.

References

[1] J.A. Wünning, J.G. Wünning, Prog. Energy Combust. Sci. 23 (1997) 81–94.
[2] C. Galletti, A. Parente, L. Tognotti, Combust. Flame 151 (2007) 649–664.
[3] A. Cavaliere, M. de Joannon, Prog. Energy Combust. Sci. 30 (2004) 329–366.
[4] A. Schuster, M. Zieba, G. Scheffknecht, J.G. Wünning, Application of FLOX technology for the utilisation of low-grade biofuels, in: Proceedings of 15th European Biomass Conference, Berlin, Germany, 2007, pp. 1703–1706.
[5] J. Leppälahti, T. Koljonen, Fuel Process. Technol. 43 (1995) 1–45.
[6] M. Becidan, Ø. Skreiberg, J.E. Hustad, Energy Fuels 21 (2007) 1173–1180.
[7] J.A. Miller, C.T. Bowman, Prog. Energy Combust. Sci. 15 (4) (1989) 287–338.
[8] N. Sullivan, A. Jensen, P. Glarborg, M.S. Day, F.F. Grcar, J.B. Bell, C. Pope, R.J. Kee, Combust. Flame 131 (2002) 285–298.
[9] P. Glarborg, A.D. Jensen, J.E. Johnson, Prog. Energy Combust. Sci. 29 (2003) 89–113.
[10] C.P. Fenimore, G.W. Jenes, J. Phys. Chem. 65 (1961) 289–303.
[11] R.P. van der Lans, P. Glarborg, K. Dam-Johansen, Prog. Energy Combust. Sci. 23 (1997) 349–377.
[12] R.P. Lindstedt, F.C. Lockwood, M.A. Selim, Combust. Sci. Tech. 99 (1994) 253–276.
[13] Ø. Skreiberg, P. Kilpinen, P. Glarborg, Combust. Flame 136 (2004) 501–518.
[14] J.F. Grcar, P. Glarborg, J.B. Bell, M.s. Day, A. Loren, A.D. Jensen, Proc. Combust. Inst. 30 (2005) 1193–1200.
[15] A. Schuster, S. Erhardt, G. Scheffknecht, J. G. Wünning, Conversion of ammonia to NO_x for flameless oxidation of low calorific value gas, in: 7th High Temperature Air Combustion and Gasification International Symposium, Phuket, Thailand, 13–16 January 2008, Ref. No. HiTACG_163.
[16] Åbo Akademi University. <http://web.abo.fi/fak/ktf/cmc/research/r_schemes.html>.
[17] P. Glarborg, K. Dam-Johansen, P. Kristensen, Final Report, Gas Research Institute, 5091-260-2126, Nordic Gas Technology Center (89-03-11), 1993.
[18] P. Glarborg, D. Kubel, P. Kristensen, J. Hansen, K. Dam-Johansen, Combust. Sci. Technol. 110–111 (1995) 461–485.
[19] J.A. Miller, P. Glarborg, Springer Series in Chemical Physics, Springer Verlag, Berlin, Germany, 1996.
[20] E. Coda Zabetta, M. Hupa, Combust. Flame 152 (2008) 14–27.
[21] E. Coda Zabetta, Modelling of nitrogen oxides in combustion at atmospheric and elevated pressures: application to biomass- and oil-derived gaseous fuels, Academic Dissertation, Painotalo Gillot Oy, Åbo, Finland, 2002.
[22] E. Coda Zabetta, P. Kilpinen, M. Hupa, K. Ståhl, J. Leppälahti, M. Cannon, J. Nieminen, Energy Fuels 14 (2000) 751–761.
[23] R. Rota, F. Bonini, A. Servida, M. Moribidelli, S. Carra, Combust. Sci. Technol. 123 (1997) 83–105.
[24] P. Kilpinen, M. Hupa, Combust. Flame 85 (1991) 94–104.
[25] B. Leckner, M. Karlsson, K. Dam-Johansen, C. Weinell, P. Kilpinen, M. Hupa, Ind. Eng. Chem. Res. 30 (1991) 2396–2404.
[26] Gas Research Institute, GRI-Mech, Ver. 3.0. <http://www.me.berkely.edu/gri-mech/>.
[27] M. Mancini, P. Schwöppe, R. Weber, S. Orsino, Combust. Flame 150 (2007) 54–59.
[28] C.K. Westbrook, Y. Mizobuchi, T.J. Poinsot, P.J. Smith, J. Warnatz, Proc. Combust. Inst. 30 (2005) 125–157.
[29] M.U. Alzueta, R. Bilbao, A. Millera, P. Glarborg, M. Østberg, K. Dam-Johansen, Energy Fuels 12 (1998) 329–338.
[30] M. Oliva, M.U. Alzueta, A. Millera, R. Bilbao, Chem. Eng. Technol. 25 (2002) 417–419.
[31] W.P. Jones, R.P. Lindstedt, Combust. Flame 73 (1988) 233–249.
[32] B.F. Magnussen, B.H. Hjertager, in: Sixteenth Symposium (International) on Combustion, The Combustion Institute, Pittsburgh, PA, 1976, pp. 719–729.
[33] M. Dean, J.W. Bozzelli, in: W.C. Gardiner (Ed.), Combustion Chemistry II, Springer-Verlag, 2000, pp. 125–341.
[34] S. Koger, H. Bockhorn, Proc. Combust. Inst. 30 (2005) 1201–1209.